ChemComm

RSC Publishing

COMMUNICATION

View Article Online
View Journal | View Issue

Cite this: *Chem. Commun.*, 2013, **49**, 2246

Received 17th December 2012,
Accepted 1st February 2013

DOI: 10.1039/c3cc38990a

www.rsc.org/chemcomm

Efficient quenching of electrochemiluminescence from K-doped graphene–CdS:Eu NCs by G-quadruplex–hemin and target recycling-assisted amplification for ultrasensitive DNA biosensing†

Hong Zhou, Yan-Yan Zhang, Jing Liu, Jing-Juan Xu* and Hong-Yuan Chen

Based on the K-doped graphene–CdS:Eu NC composites and the nicking endonuclease (NEase) assisted strand-scission cycle, we have developed an ultrasensitive and selective electrochemiluminescence (ECL) DNA biosensor using the G-quadruplex–hemin-based DNAzyme which acts as an electrocatalyst for the reduction of H_2O_2, the coreactant of CdS:Eu NCs ECL.

Detection of specific DNA sequences at ultralow concentration is of great significance in clinical diagnostics, environmental monitoring, gene therapy, and a variety of other biomedical applications.[1] Many approaches based on various target amplification and signal amplification principles have thus been developed, such as polymerase chain reaction (PCR)[2] and rolling circle amplification (RCA).[3] However, these methods suffer from several drawbacks including complex handling procedures, vulnerability to cross-contamination and high cost. Therefore, the nicking endonuclease signal amplification (NESA) as a newly developed technique attracted researchers' attention to design sensitive biosensors of target DNA for their autonomous circular amplification and simple operations.[4] Moreover, different electrochemical and optical DNA sensing techniques have also been developed for the rapid, selective and sensitive analysis of DNA.[5] Among them the electrochemiluminescence (ECL) technique, offering a lot of advantages such as low cost, wide range of analytes, low background signal and high sensitivity, has recently become an important and powerful analytical tool.[6]

Recently, semiconductor nanocrystal (NC)-based ECL, which is usually generated with cathodic emission in the presence of different coreactants such as oxygen, hydrogen peroxide or peroxydisulfate, has been used for the development of ECL biosensors.[7] Subsequently, some new NC nanostructures have been developed to improve the ECL intensity and biocompatibility, such as NC composites with carbon nanotubes, nanogold, dendrimers, graphene oxide, *etc.*[8] Catalytic nucleic acids (DNAzymes), which are a kind of artificial enzyme that exhibits surprising potential as a new biocatalyst, has intrigued researchers as catalytic amplifiers in biorecognition and biosensing events.[9] As one of the most interesting DNAzymes, G-quadruplex–hemin DNAzyme, which is composed of a single-stranded guanine-rich nucleic acid and hemin, has horseradish peroxidase-like activity and shows great catalytic activity to H_2O_2. Therefore, it has shown considerable potential as a novel kind of catalytic label for the development of various DNA biosensors.

In the present study, an ECL method for amplified detection of DNA based on K-doped graphene–CdS:Eu NC composites and the nicking endonuclease (NEase) assisted strand-scission cycle was developed. As shown in Scheme 1, we prepared novel K-doped graphene–NC (K-GR–NC) composites *via* electrostatic interactions between negatively charged 3-mercaptopropionic acid (MPA) modified CdS:Eu NCs and positively charged graphene, which was noncovalently functionalized with poly(diallyldimethylammonium chloride) (PDDA) *via* electrostatic interactions. Our previous work observed that the alkali metal K-doped graphene could enhance the rate of electron transfer and the sensitivity in biosensing applications.[10] Obviously, one can expect the interesting use of this new K-doped graphene for enhancing the NC-ECL performance. And we also successfully demonstrated that Eu^{3+} ions could alter the surface of CdS NCs and create a new surface state-Eu^{3+} complex, resulting in a large enhancement in the ECL intensity.[11] Here, the K-doped graphene nanomaterials can effectually increase the surface area and meanwhile improve

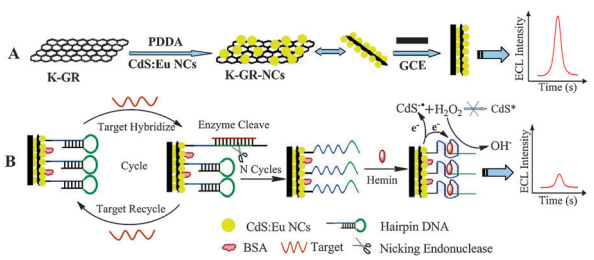

Scheme 1 Schematic representation of the proposed ECL-DNA biosensor.

State Key Laboratory of Analytical Chemistry for Life Science, School of Chemistry and Chemical Engineering, Nanjing University, Nanjing 210093, China. E-mail: xujj@nju.edu.cn; Fax: +86-25-83597294; Tel: +86-25-83597294

† Electronic supplementary information (ESI) available: Experimental details. See DOI: 10.1039/c3cc38990a

the electron transfer at the electrode interface (Fig. S1, ESI†). So the layer-by-layer assembly K-GR–NC composites film on the glassy carbon electrode (GCE) not only improved the ECL intensity, but also provided a large specific surface for high levels of DNA loading, which resulted in extreme sensitivity. Subsequently, a hairpin DNA containing the single-stranded loop which was complementary to the target analyte DNA was immobilized on the K-GR–NC composites film on the GCE.

In our detection system, the NEase is specifically designed to recognize specific nucleotide sequences in double-stranded DNA (dsDNA) and cleaves only one of the two strands. Therefore, in the absence of target DNA, the NEase cannot nick the hairpin DNA and a part of the G-rich nucleic acid sequence yields a stable duplex domain in the stem region of the hairpin which eliminates the formation of the active G-quadruplex–hemin structure when the hemin and K^+ are added in the test system. However, when a perfectly matched target DNA hybridizes to the hairpin DNA, the stem of the hairpin DNA is opened and a full recognition site will form for the NEase. Then the NEase binds to and nicks the cleavage site. After nicking, the hairpin DNA is cleaved into two fragments, and only the G-rich sequence remains on the electrode surface. Subsequently, the released target DNA can hybridize with a new un-nicked hairpin DNA and initiate the second cycle of cleavage. Eventually, each target strand is recycled into solution, resulting in the cleavage of many hairpin DNA. Upon completion of the strand-scission cycle, only the G-rich fragments remain on the electrode surface. Therefore, a G-quadruplex–hemin DNAzyme could form with the help of the hemin and K^+, which electrocatalyze the reduction of H_2O_2, the coreactant for cathodic ECL emission, leading to an obvious decrease in ECL intensity. In this way, a single target can activate many DNAzymes. The activated G-quadruplex–hemin DNAzyme on the electrode surface has strong electrocatalytic activity for quenching the ECL emission leading to the amplification detection of target DNA.

Fig. 1A shows the TEM image of CdS:Eu NCs. According to the TEM observation, the average size of the CdS:Eu NCs was about 6 nm. Fig. 1B and C show the SEM images of K-doped graphene (K-GR) and K-GR–NC composites. From Fig. 1C, it was observed that there was homogeneous and dense coverage of CdS:Eu NCs on the surface of the K-GR. The composition of K-GR–NC composites was further confirmed by means of selected area energy dispersive X-ray analysis (SAEDX, Fig. 1D), UV-vis absorption spectrum and Raman spectra (Fig. S2A and B, ESI†). The result revealed the identity of the CdS:Eu NCs coupled onto the K-GR sheets.

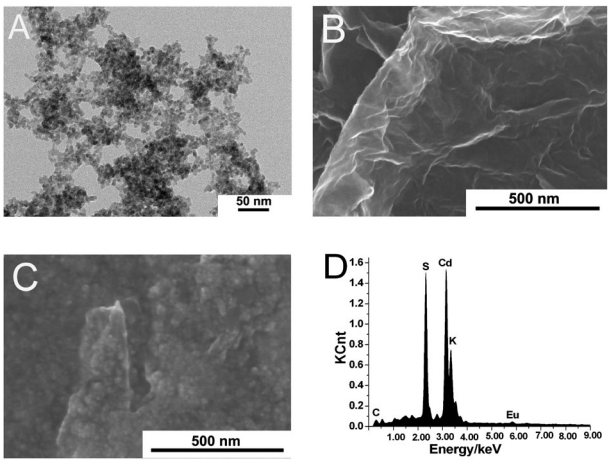

Fig. 1 TEM images of CdS:Eu NCs (A); SEM images of K-GR (B) and K-GR–NCs composites (C); the SAEDX analysis of K-GR–NC composites (D).

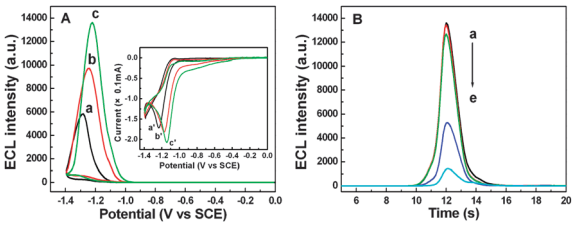

Fig. 2 (A) The ECL–potential curves of the CdS:Eu NC electrodes (a), GR–NC composite electrodes (b) and K-GR–NC composite electrodes (c), inset: the corresponding cyclic voltammograms (CVs): a′ to a; b′ to b; c′ to c. (B) ECL intensity – time behavior of hairpin DNA probe/NCs/GCE (a); the electrode (a) in the presence of NEase and hemin, but without target DNA (b); the electrode (a) in the presence of target DNA and NEase, but without hemin (c); the electrode (a) in the presence of target DNA and hemin, but without NEase (d); the electrode (a) in the presence of target DNA, NEase and hemin (e). Experimental conditions: target DNA, 8.0 pM; NEase, 0.5 U μL^{-1}; hemin, 1.0 μM; ECL detection buffer: 0.1 M PBS (pH 8.5) containing 0.1 M KCl and 5.0 mM H_2O_2. Scan rate, 100 mV s^{-1}.

As shown in Fig. 2A, curves a, b and c depict the ECL-potential curves of the pure CdS:Eu NCs, GR–NC composites and K-GR–NC composite films, respectively. Obviously, the K-GR–NC nanocomposites could decrease the reduction potential of CdS:Eu NCs and H_2O_2 (Fig. 2A, the inset curve c′) and greatly enhance the ECL intensity (Fig. 2A, curve c), and a much lower ECL enhancement in the employment of ordinary graphene (curve b) was observed in the control experiment. The reasons for this are that the K-doped graphene not only acted as a conducting substrate effectively reducing the injection barrier of electrons to CdS:Eu NCs in ECL reaction but also anchored more CdS:Eu NCs due to its high specific surface area. Electrochemical impedance spectroscopy (Fig. S3, ESI†) and ECL signals at each immobilization step were recorded to characterize the feasibility of this ECL biosensor. As shown in Fig. 2B, under the optimization of experimental conditions (Fig. S4, ESI†), the hairpin DNA probe/NCs/GCE showed a strong cathodic ECL emission in the presence of coreactant H_2O_2 (curve a). In the presence of NEase and hemin, but without target DNA, or in the presence of target DNA and NEase, but without hemin, there was no significant change in ECL intensity (curves b and c), indicating that there was no G-quadruplex–hemin formed. Upon contact with the target DNA and hemin but without NEase, there was a visible decrease in ECL intensity (curve d). The reason was that the stem of the hairpin DNA was opened and the active G-quadruplex–hemin structure formed, which electrocatalytically reduced H_2O_2, the coreactant for cathodic ECL emission, leading to an obvious decrease in ECL intensity. After adding NEase and nicking reaction, the ECL peak height decreased by 91% (curve e), indicating that a number of G-quadruplex–hemin DNAzymes formed with the

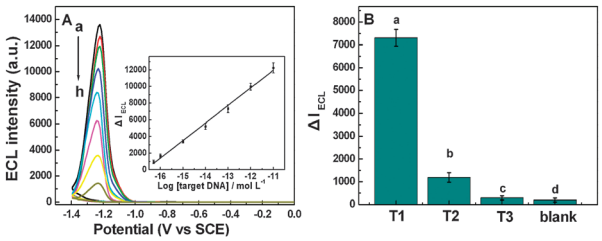

Fig. 3 (A) ECL signal response for detection of different concentrations of target DNA. The concentrations of the target DNA: (a) 0, (b) 50 aM, (c) 100 aM, (d) 1 fM, (e) 10 fM, (f) 100 fM, (g) 1 pM, and (h) 10 pM. Inset: linear relationship between relative ECL intensity (ΔI) and the logarithm of target DNA concentration, three measurements for each point. (B) ECL signals for 0.1 pM of different DNA sequences: (a) complementary sequence (target DNA), (b) single-base-mismatched sequence, (c) noncomplementary sequence, and (d) blank. Three measurements for each point.

help of the nicking endonuclease and hemin, which electrocatalytically reduced H_2O_2, leading to a significant decrease in ECL intensity. And the mechanism of the proposed ECL DNA biosensor is shown in ESI.†

The sensitivity of the assay based on K-doped graphene–CdS:Eu NC composites and the NEase assisted strand-scission cycle was investigated by varying the target concentration. As displayed in Fig. 3A, the intensity of ECL was very sensitive to the change in the target DNA concentration and decreased with the increase in the concentration of target DNA ranging from 0 aM to 10 pM, and the ECL decrement ΔI ($\Delta I = I_0 - I$) was found to be logarithmically related to the concentration of target DNA in the range from 50 aM to 10 pM (R = 0.997, the inset in Fig. 3A). The detection limit is experimentally found to be 50 aM, which is superior to those obtained from other methods.[12] This may be attributed to the following factors: low background of ECL assay and the K-GR nanomaterials which could increase the surface area and improve the electron transfer at the electrode interface. Moreover, the possibility of reusing target molecules based on a nicking enzyme reaction greatly magnifies the detection signal.

In this biosensor, the specificity was investigated with the same concentration of complete complementary target DNA sequences (T1), the one-base mismatched DNA sequences (T2), the non-complementary DNA sequences (T3) and blank (without DNA), respectively. As shown in Fig. 3B, the highest ECL decrement (ΔI) was observed after hybridization with T1 (a). However, when hybridized with T2, the ECL decrement increased slightly (b), and the T3 showed small change (c) compared to the blank (d). We also found that the DNA with one base mismatch at the binding or nicking site led to a slight increase in the ECL decrement compared with T1. These results indicate that the developed assay could exhibit an excellent specificity to distinguish the single-base mismatched DNA target, which benefits from using the stem-loop DNA probe as the sensing component. The reproducibility of this ECL biosensor was evaluated from the response to 10 fM target DNA at five electrodes. A series of measurements resulted in an interassay relative standard deviation (R.S.D) of 8.17%, indicating satisfactory biosensor-to-biosensor reproducibility of the fabrication protocol.

In summary, a simple, label-free, ultrasensitive and selective DNA biosensor based on K-doped graphene–CdS:Eu NC composites and the nicking endonuclease (NEase) assisted strand-scission cycle has been developed. With advantages such as simple preparation, convenient operation, wide linear range, high sensitivity and good selectivity, this strategy has the potential to be integrated in portable, low-cost and simplified devices for diagnostic applications.

This work was supported by the 973 Program (2012CB932600, 2013CB933800), the National Natural Science Foundation (No. 21025522 and 21135003) and the National Natural Science Funds for Creative Research Groups (21121091) of China.

Notes and references

1 (*a*) J. Huang, Y. R. Wu, Y. Chen, Z. Zhu, X. H. Yang, C. Y. J. Yang, K. M. Wang and W. H. Tan, *Angew. Chem., Int. Ed.*, 2011, **50**, 401–404; (*b*) H. F. Dong, W. C. Gao, F. Yan, H. X. Ji and H. X. Ju, *Anal. Chem.*, 2010, **82**, 5511–5517.
2 (*a*) Z. Cheglakov, Y. Weizmann, M. K. Beissenhirtz and I. Willner, *Chem. Commun.*, 2006, 3205–3207; (*b*) A. Marx and M. Strerath, *Angew. Chem., Int. Ed.*, 2005, **44**, 7842.
3 (*a*) W. Zhao, M. M. Ali, M. A. Brook and Y. Li, *Angew. Chem., Int. Ed.*, 2008, **47**, 6330–6337; (*b*) S. Bi, L. Li and S. S. Zhang, *Anal. Chem.*, 2010, **82**, 9447–9454.
4 (*a*) J. J. Li, Y. Chu, B. Y. Lee and X. S. Xie, *Nucleic Acids Res.*, 2008, **36**, e36; (*b*) B. J. Zou, Y. J. Ma, H. P. Wu and G. H. Zhou, *Angew. Chem., Int. Ed.*, 2010, **49**, 1–5; (*c*) J. H. Chen, J. Zhang, J. Li, F. F. Fu, H.-H. Yang and G. N. Chen, *Chem. Commun.*, 2010, **46**, 5939–5941.
5 (*a*) N. L. Rosi and C. A. Mirkin, *Chem. Rev.*, 2005, **105**, 1547–1562; (*b*) W.-W. Zhao, J. Wang, J.-J. Xu and H.-Y. Chen, *Chem. Commun.*, 2011, **47**, 10990–10992; (*c*) S. Alwarappan, K. Cissel, S. Dixit, C.-Z. Li and S. Mohapatra, *J. Electroanal. Chem.*, 2012, **686**, 69–72.
6 (*a*) H. Zhou, J. Liu, J.-J. Xu and H.-Y. Chen, *Chem. Commun.*, 2011, **47**, 8358–8360; (*b*) Y. Shan, J.-J. Xu and H.-Y. Chen, *Chem. Commun.*, 2009, 905–907; (*c*) C.-Y. Tian, J.-J. Xu and H.-Y. Chen, *Chem. Commun.*, 2012, **48**, 8234–8236; (*d*) Y. Shan, J.-J. Xu and H.-Y. Chen, *Chem. Commun.*, 2010, **46**, 4187–4189.
7 (*a*) D. J. Lin, J. Wu, F. Yan, S. Y. Deng and H. X. Ju, *Anal. Chem.*, 2011, **83**, 5214–5221; (*b*) G. F. Jie, L. Wang and S. S. Zhang, *Chem.–Eur. J.*, 2011, **17**, 641–648; (*c*) J. Wang, Y. Shan, W.-W. Zhao, J.-J. Xu and H.-Y. Chen, *Anal. Chem.*, 2011, **83**, 4004–4011.
8 (*a*) X.-F. Wang, Y. Zhou, J.-J. Xu and H.-Y. Chen, *Adv. Funct. Mater.*, 2009, **19**, 1444–1450; (*b*) H. Zhou, J. Liu, J.-J. Xu and H.-Y. Chen, *Anal. Chem.*, 2011, **83**, 8320–8328; (*c*) F. Divsar and H. X. Ju, *Chem. Commun.*, 2011, **47**, 9879–9881; (*d*) L.-L. Li, K.-P. Liu, G.-H. Yang, C.-M. Wang, J.-R. Zhang and J.-J. Zhu, *Adv. Funct. Mater.*, 2011, **21**, 869–878.
9 I. Willner, B. Shlyahovsky, M. Zayats and B. Willner, *Chem. Soc. Rev.*, 2008, **37**, 1153–1165.
10 (*a*) X.-R. Li, F.-Y. Kong, J. Liu, J.-J. Xu and H.-Y. Chen, *Adv. Funct. Mater.*, 2012, **22**, 1981–1988; (*b*) J. Wang, W.-W. Zhao, X.-R. Li, J.-J. Xu and H.-Y. Chen, *Chem. Commun.*, 2012, **48**, 6429–6431.
11 (*a*) L. Deng, Y. Shan, J.-J. Xu and H.-Y. Chen, *Nanoscale*, 2012, **4**, 831–836; (*b*) H. Zhou, Y.-Y. Zhang, J. Liu, J.-J. Xu and H.-Y. Chen, *J. Phys. Chem. C*, 2012, **116**, 17773–17780.
12 (*a*) K. W. Hsieh, Y. Xiao and H. T. Soh, *Langmuir*, 2010, **26**, 10392–10396; (*b*) S. Bi, L. Li and Y. Y. Cui, *Chem. Commun.*, 2012, **48**, 9879–9881; (*c*) S. J. He, K.-K. Liu, S. Su, J. Yan, X. H. Mao, D. F. Wang, Y. He, L.-J. Li, S. P. Song and C. H. Fan, *Anal. Chem.*, 2012, **84**, 4622–4627.

